HHS Public Access

Author manuscript

Nat Microbiol. Author manuscript; available in PMC 2017 June 05.

Published in final edited form as:

Nat Microbiol. ; 2: 16232. doi:10.1038/nmicrobiol.2016.232.

Mycobacterium tuberculosis EsxH inhibits ESCRT-dependent CD4+ T-cell activation

Cynthia Portal-Celhay[1], **JoAnn M. Tufariello**[2,3], **Smita Srivastava**[1], **Aleena Zahra**[1], **Thais Klevorn**[1], **Patricia S. Grace**[1], **Alka Mehra**[1], **Heidi S. Park**[1], **Joel D. Ernst**[1], **William R. Jacobs Jr**[2,4,‡,⋆], and **Jennifer A. Philips**[1,†,‡,⋆]

[1]Division of Infectious Diseases, Department of Medicine, New York University School of Medicine, New York, New York 10016, USA

[2]Department of Microbiology and Immunology, Albert Einstein College of Medicine, Bronx, New York 10461, USA

[3]Center for Microbial Pathogenesis, Institute for Biomedical Sciences, Georgia State University, Atlanta, Georgia 30303, USA

[4]Howards Hughes Medical Institute, Albert Einstein College of Medicine, Bronx, New York 10461, USA

Abstract

Mycobacterium tuberculosis (Mtb) establishes a persistent infection, despite inducing antigen-specific T-cell responses. Although T cells arrive at the site of infection, they do not provide sterilizing immunity. The molecular basis of how Mtb impairs T-cell function is not clear. Mtb has been reported to block major histocompatibility complex class II (MHC-II) antigen presentation; however, no bacterial effector or host-cell target mediating this effect has been identified. We recently found that Mtb EsxH, which is secreted by the Esx-3 type VII secretion system, directly inhibits the endosomal sorting complex required for transport (ESCRT) machinery. Here, we showed that ESCRT is required for optimal antigen processing; correspondingly, overexpression and loss-of-function studies demonstrated that EsxH inhibited the ability of macrophages and dendritic cells to activate Mtb antigen-specific $CD4^+$ T cells. Compared with the wild-type strain, the *esxH*-deficient strain induced fivefold more antigen-specific $CD4^+$ T-cell proliferation in the mediastinal lymph nodes of mice. We also found that EsxH undermined the ability of effector

⋆Correspondence and requests for materials should be addressed to W.R.J. and J.A.P. philips.j.a@wustl.edu; jacobsw@hhmi.org.
†Present address: Division of Infectious Diseases, Department of Medicine, Washington University School of Medicine, St Louis, Missouri 63110, USA
‡These authors contributed equally to this work.

Author contributions

C.P.-C., and J.A.P. conceived and designed the study. C.P.-C. performed all the *in vitro* experiments with help from T.K., with the exception of the trafficking studies done by A.Z. C.P.-C. and S.S. designed and performed *in vivo* experiments. A.M. and H.S.P. created plasmids. J.M.T. and W.R.J. contributed the Δ*esxH* and Δ*pe5-ppe4* strains. C.P.-C. and P.S. G performed flow cytometry. C.P.-C. and J.A.P. interpreted the results and wrote the manuscript. J.D.E., W.R.J. and J.A.P. oversaw the project.

Additional information

Supplementary information is available for this paper. Reprints and permissions information is available at www.nature.com/reprints.

Competing interests

The authors declare no competing financial interests.

$CD4^+$ T cells to recognize infected macrophages and clear Mtb. These results provide a molecular explanation for how Mtb impairs the adaptive immune response.

Host defences, both innate and adaptive, are subverted by *Mycobacterium tuberculosis* (Mtb). During Mtb infection, there is a delay in priming antigen-specific $CD4^+$ and $CD8^+$ cells by dendritic cells (DCs) in the lymph node[1]. When the effector $CD4^+$ T cells traffic to the site of infection in the lungs, although they promote the antimycobacterial activity of macrophages by secreting cytokines such as interferon (IFN)-γ[2], they fail to generate sterilizing immunity. Currently, we lack a comprehensive and detailed understanding as to why major histocompatibility complex class II (MHC-II) antigen presentation fails during Mtb infection. In naive macrophages, Mtb can act through Toll-like receptor 2 to block IFN-γ-induced MHC-II transcription[3–5], although the contribution this plays *in vivo* is unclear[6]. How Mtb impairs antigen presentation in macrophages already expressing MHC-II is less well understood. One proposed mechanism is that by blocking phagosome maturation Mtb impairs efficient processing of antigen and the MHC-II-associated invariant chain[7,8]. However, there have been contradictory results regarding the impact of phagosome maturation on antigen presentation[8–11]. Contradictory results have also been reported in DCs. Some studies have demonstrated that Mtb inhibits DCs maturation, thereby impairing mobilization of MHC-II molecules to the cell surface[12], whereas others have shown that Mtb upregulates DC expression of MHC-II, co-stimulatory molecules and inflammatory cytokines[13,14]. More recent data have shown that Mtb-infected DCs are inefficient at priming antigen-specific $CD4^+$ T cells[15–17]. Rather, bystander uninfected cells take up Mtb antigen and prime $CD4^+$ T cells[18,19].

Our group recently found that Mtb EsxH inhibits phagosome maturation by targeting the host endosomal sorting complex required for transport (ESCRT)[20]. EsxH forms a heterodimer with EsxG ($EsxGH_{Mt}$), which is secreted by the Esx-3 type VII secretion system. $EsxGH_{Mt}$ is involved in iron and zinc acquisition[21–25], and recent work has demonstrated that $EsxGH_{Mt}$ also plays an additional role in virulence[20,26,27]. $EsxGH_{Mt}$ binds the host protein hepatocyte growth factor-regulated tyrosine kinase substrate (HGS, also known as HRS), a component of the ESCRT machinery[20]. ESCRT plays a well-described role in directing cell-surface receptors into intraluminal vesicles of multivesicular bodies so they can be degraded in the lysosome[28]. We found that ESCRT is also required for phagosome maturation[20,29], and we hypothesized that ESCRT, and by extension $EsxGH_{Mt}$, regulates MHC-II antigen presentation. In this study, we showed that ESCRT promotes T-cell activation during Mtb infection by facilitating antigen processing. We demonstrated that $EsxGH_{Mt}$ impairs the ability of macrophages and DCs to present mycobacterial antigens and activate $CD4^+$ T cells, resulting in impaired T-cell priming and defective effector function. Overall, our data support a model in which EsxH inhibits ESCRT, thereby undermining two key aspects of the adaptive immune response: (1) efficient priming of naive T cells, and (2) recognition of Mtb-infected cells by $CD4^+$ T cells.

Results

ESCRT promotes antigen presentation during Mtb infection

To test the hypothesis that ESCRT contributes to antigen presentation, we depleted HRS and TSG101, components of ESCRT-0 and ESCRT-I, from bone marrow-derived macrophages (BMDMs) (Fig. 1a). Following ESCRT depletion, BMDMs were activated with IFN-γ to induce MHC-II expression and infected the following day with Mtb. The ability of the infected macrophages to activate $CD4^+$ T cells was assessed using T-helper 1 (T_H1) polarized $CD4^+$ effector cells that express a transgenic T-cell antigen receptor (TCR-Tg) specific for peptide 25 (amino acids 240–254) of Mtb Ag85B protein (P25TCR-Tg T_H1 cells)[30], which secrete IFN-γ when co-cultured with Mtb-infected BMDMs. We found that macrophages depleted of HRS or TSG101 were poor at stimulating P25TCR-Tg effector $CD4^+$ T cells, inducing 30% less IFN-γ release than control cells (Fig. 1b). Similar findings were observed with $CD4^+$ T_H1 cells specific for another prominent secreted antigen of Mtb, EsxA/ESAT-$6_{3–15}$ (C7TCR-Tg T_H1 cells; Fig. 1c). IFN-γ production by P25 and C7 TCR T_H1 cells was antigen specific, as IFN-γ was not made following co-culture with macrophages infected with Ag85B- or ESAT-6-null strains of Mtb (Δ*fpbB* and Δ*esxA*; Fig. 1b,c). Importantly, multiple independent small interfering RNAs (siRNA) targeting *Tsg101* or *Hrs* impaired the ability of infected macrophages to stimulate T cells (Supplementary Fig. 1a–c), and the degree of HRS depletion correlated with levels of impairment in T-cell activation (Supplementary Fig. 1b,c). At the maximal HRS depletion that we were able to achieve, approximately 20% of HRS protein remained, and IFN-γ production was suppressed by approximately 40%. These results indicated that ESCRT promotes the ability of macrophages to activate Mtb-specific $CD4^+$ effector T cells.

ESCRT facilitates antigen processing by macrophages

The role of ESCRT in antigen presentation has not been studied. In DCs, cell-surface levels of MHC-II are regulated by ubiquitin-dependent sorting to lysosomes[31,32], suggesting that ESCRT might control MHC-II trafficking in DCs, although this has not been tested directly. Whether ESCRT would play a similar role in BMDMs is unclear. To assess this directly, we compared cell-surface MHC-II levels between control BMDMs and those depleted of HRS or TSG101. We found no difference, regardless of infection status, when assayed by flow cytometry (Fig. 2a). It is also possible that, by controlling the multivesicular architecture of the MHC-II compartment or promoting phagosome maturation[20,29], ESCRT might influence antigen processing or loading. We found that ESCRT-depleted BMDMs were impaired for activating P25TCR-Tg $CD4^+$ effector T cells in the presence of exogenously added recombinant Ag85B, but behaved similarly to controls when peptide 25 was used as the antigen (Fig. 2b), suggesting that the defect is at the level of processing the protein into peptide. To evaluate this further, we used DQ-OVA, a self-quenched conjugate of ovalbumin that exhibits bright green fluorescence on proteolytic degradation (Fig. 2c). Quantification of fluorescence indicated that ESCRT silencing impaired the degradation of ovalbumin (Fig. 2d). From these experiments, we concluded that ESCRT promotes antigen presentation by facilitating antigen processing.

ESCRT does not restrict bacterial growth in IFN-γ-activated macrophages

Although Mtb arrests phagosome maturation, in naive macrophages a fraction of the bacilli are delivered to the lysosome, which we previously showed depends on ESCRT[20]. As IFN-γ partially overcomes the arrest in phagosome maturation imposed by Mtb[33–35], we asked whether ESCRT is also involved in phagosome maturation in IFN-γ-activated macrophages, which we used for the antigen presentation assays. As we reported previously, silencing of *Tsg101* and *Hrs* in naive macrophages did not decrease the total lysosomal-associated membrane protein 1 (LAMP1) signal but led to diminished co-localization between Mtb and LAMP1 (a marker of late endosomes and lysosomes) and enhanced intracellular bacterial growth when compared with control cells (Supplementary Fig. 2a,c,d)[20]. Surprisingly, in IFN-γ-activated macrophages, the same silencing had no effect on the co-localization of bacteria with LAMP1 or on bacterial survival (Supplementary Fig. 2b–d). Thus, phagolysosomal maturation and control of Mtb replication is largely independent of ESCRT in IFN-γ-activated macrophages. Therefore, the impairment in antigen presentation seen with ESCRT silencing is not due to an overall difference in bacterial degradation.

Antigen presentation is impaired by Mtb $EsxGH_{Mt}$ but not by *Mycobacterium smegmatis* EsxGH

As $EsxGH_{Mt}$ disrupts ESCRT[20], we wondered whether $EsxGH_{Mt}$ impairs antigen presentation. We found that macrophages infected with a Δ*esxH* mutant elicited 50% more T-cell activation compared with BMDMs infected with wild-type Mtb, as assessed by IFN-γ production (Fig. 3 a). Bone marrow-derived DCs (BMDCs) showed an even more pronounced effect, as infection with the Δ*esxH* mutant resulted in a greater than threefold enhancement in T-cell activation (Fig. 3b). In both cases, the increase in T-cell activation was largely reversed by genetic complementation. The enhanced response was not due to more Ag85B secretion from the mutant (Fig. 3c). While the Δ*esxH* mutant requires exogenous siderophore to grow on solid medium, it is only modestly impaired in liquid medium[26], and there was no difference in the intracellular survival of the wild type and Δ*esxH* at the time the antigen presentation assay was performed (Fig. 3d). Furthermore, when ESCRT was silenced, the Δ*esxH* mutant stimulated P25 T cells to a similar extent as control cells infected with wild-type Mtb (Fig. 3e), consistent with the idea that *esxH* impairs antigen presentation by inhibiting HRS. IFN-γ release was greatest in magnitude in the case of control cells infected with the Δ*esxH* mutant, whereas it was least in the context of ESCRT-silenced cells infected with Mtb strain H37Rv. The inhibition of IFN-γ by H37Rv relative to Δ*esxH* seen in ESCRT-silenced cells might reflect the fact that RNA interference (RNAi)-mediated silencing fails to fully deplete the target protein and that $EsxGH_{Mt}$ expression does not fully inhibit ESCRT. Alternatively, $EsxGH_{Mt}$ may have additional targets beyond HRS that suppress antigen presentation.

To test whether additional $EsxGH_{Mt}$ expressed from Mtb could further inhibit antigen presentation, we examined a wild-type strain that contained *esxGH*$_{Mt}$ on a plasmid[20]. Macrophages infected with the $EsxGH_{Mt}$-overexpressing Mtb strain elicited decreased activation of P25 $CD4^+$ T cells compared with those infected with a strain containing the vector (Fig. 3f). In addition, when Mtb contained a plasmid bearing $EsxGH_{Ms}$, the *M. smegmatis* homologue of $EsxGH_{Mt}$, which does not inhibit ESCRT[20], there was no effect on

antigen presentation (Fig. 3f). The degree of inhibition was comparable if Mtb overexpressed $EsxGH_{Mt}$ or if ESCRT was silenced in the BMDMs (Fig. 3g). Infecting ESCRT-depleted macrophages with the Mtb strain overexpressing $EsxGH_{Mt}$ did not result in an additive defect in T-cell activation beyond that seen with either manipulation alone. This is consistent with the idea that $EsxGH_{Mt}$ and siRNAs depleting HRS and TSG101 target a common pathway required for antigen presentation. In cells in which *Tsg101* or *Hrs* were silenced, there was no statistically significant difference in T-cell activation between infection with the vector control strain and the overexpressing strain, although there was a trend towards a small decrease from the overexpressing strain. In macrophages infected by Mtb overexpressing $EsxGH_{Mt}$, *Hrs* silencing resulted in a small but statistically significant decrease in IFN-γ production relative to macrophages treated with control siRNA. These small decreases associated with the combination of the overexpressing strain and ESCRT silencing might be because RNAi-mediated silencing and $EsxGH_{Mt}$ do not fully inhibit Hrs or because $EsxGH_{Mt}$ has additional targets. Overall, we concluded that both overexpression and loss-of-function studies indicated that $EsxGH_{Mt}$ impairs effector T-cell responses, similar to the situation seen with ESCRT silencing.

Antigen presentation is unaffected by PE5 and EsxA

In addition to containing *esxG* and *esxH*, the *esx-3* locus encodes *pe5* and *ppe4*, members of the proline-glutamic acid (PE) and proline–proline–glutamic acid (PPE) families, respectively. Tufariello *et al.*[26] showed that PE5 is secreted by Esx-3, and, like the Δ*esxH* mutant, Δ*pe5-ppe4* requires exogenous siderophore-bound iron to grow on solid medium. In addition, the Δ*esxH* mutant fails to secrete PE5, raising the possibility that PE5 is responsible for the phenotype of the Δ*esxH* mutant. However, unlike Δ*esxH*, the Δ*pe5-ppe4* mutant did not result in increased T-cell responses (Fig. 3a,b). Thus, the influence of EsxH on antigen presentation is not explained by its role in iron acquisition or its effect on PE5 secretion. We also tested the role of EsxA, which is secreted by the Esx-1 type VII secretion system. Macrophages and DCs infected with the Δ*esxA* mutant did not showed increased ability to activate T cells (Fig. 3a,b), corroborating the idea that enhanced antigen presentation does not simply reflect bacterial attenuation.

$EsxGH_{Mt}$ impairs priming of naive $CD4^+$ T cells *in vivo*

We hypothesized that $EsxGH_{Mt}$ might contribute to impaired priming of $CD4^+$ T cells *in vivo*. To test this hypothesis, we adoptively transferred carboxyfluorescein succinimidyl ester (CFSE)-labelled P25TCR-Tg $CD4^+$ T cells into CD45.2 congenie mice and infected them by aerosol with H37Rv or the Δ*esxH* mutant and assessed the proliferation of P25TCR-Tg $CD4^+$ T cells in the mediastinal lymph nodes (MLNs) and lungs. In initial experiments using an inoculum of 10^2–10^3 colony-forming units (c.f.u.), Δ*esxH* was cleared from the lungs and failed to disseminate to the draining lymph node. When we used high-dose Δ*esxH* (10^4 c.f.u.), the bacteria disseminated to the MLNs (Fig. 4a), although the number of c.f.u. in the lung was much lower than that found in mice infected with 10^2 c.f.u. H37Rv, and there were orders of magnitude fewer Δ*esxH* mutant in the MLNs than H37Rv at 14 d postinfection. Proliferation of the P25TCR-Tg $CD4^+$ T cells in the MLNs was observed at this time point in response to both Δ*esxH* and H37Rv (Fig. 4b), and a similar percentage of P25TCR-Tg $CD4^+$ T cells proliferated in the MLNs and lungs in response to

both strains (Fig. 4c). That this degree of T-cell proliferation occurred in response to orders of magnitude fewer Δ*esxH* bacilli in the MLNs suggested that Δ*esxH*-infected cells might be superior to wild-type Mtb-infected cells in priming $CD4^+$ T cells.

To compare P25TCRTg $CD4^+$ T-cell responses with equal numbers of wild-type and Δ*esxH* mutant *in vivo*, we used intratracheal transfer of infected BMDCs. We adoptively transferred naive CFSE-labelled P25TCRTg $CD4^+$ T cells in MHC-II knockout (*MHC-II*$^{-/-}$) mice and compared their activation following intratracheal transfer of MHC-II-expressing (wild-type) BMDCs infected with equal numbers of H37Rv or Δ*esxH*. This experimental design allowed us to assay the contribution of antigen presentation from the infected DCs and eliminated the possibility that antigen transfer to uninfected bystander DCs was contributing to T-cell priming. Analysis of mediastinal MLNs revealed that, following transfer of DCs infected with Δ*esxH*, there was a threefold increase in the number of P25TCR-Tg $CD4^+$ T cells (Fig. 5a,b) and five- to six-fold more P25TCR-Tg $CD4^+$ T-cell proliferation (Fig. 5c,d). This enhanced $CD4^+$ T-cell priming was not due to a higher bacterial burden, as both groups of infected DCs contained similar numbers of bacteria, and equivalent numbers of DCs were transferred into recipient animals (Fig. 5e). There was also no difference in the number of bacteria in the lungs of the recipient mice (Fig. 5f). Interestingly, and consistent with the aerosol experiment above, the MLNs contained approximately half as many Δ*esxH* mutant as wild-type bacteria (Fig. 5g) but led to a fivefold increase in $CD4^+$ T-cell proliferation. Thus, following transfer of infected DCs, there was more T-cell proliferation in response to fewer Δ*esxH* than wild-type bacilli. We concluded that EsxH impairs the ability of Mtb-infected DCs to prime $CD4^+$ T cells *in vivo*.

EsxH protects Mtb from $CD4^+$ T-cell-mediated killing

Direct recognition of infected macrophages is important for $CD4^+$ T cells to control Mtb[36]. To determine whether EsxH impairs the ability of effector $CD4^+$ T cells to recognize infected macrophages, we cocultured BMDMs infected with either wild-type Mtb or the Δ*esxH* mutant with and without P25TCR-Tg $CD4^+$ T cells and plated them to determine the number of c.f.u. We found that the addition of P25TCR-Tg $CD4^+$ T cells to naive or IFN-γ-activated BMDMs had a modest effect on Mtb growth if macrophages were infected with wild-type Mtb (Fig. 6a,b). In contrast, addition of effector T cells to macrophages infected with the Δ*esxH* mutant resulted in substantial bacterial killing (Fig. 6a,b). We concluded that EsxH limits the ability of T cells to promote clearance of Mtb from infected macrophages. The enhanced sensitivity to T cells exhibited by the Δ*esxH* mutant may also explain why there were fewer Δ*esxH* than wild-type bacilli in the MLNs in the DC transfer experiments above (Fig. 5g), while in the lungs Δ*esxH* and wild type were no different (Fig. 5f). To test whether EsxH protected Mtb from T-cell-facilitated killing *in vivo*, we compared the bacterial burden of the Δ*esxH* mutant in the lungs of C57BL/6 and *MHC-II*$^{-/-}$ mice, which lack $CD4^+$ T cells. Attenuation of the Δ*esxH* mutant was ameliorated in *MHC-II*$^{-/-}$ mice; in wild-type mice, there was more than a 4-log difference in c.f.u. between Δ*esxH* and wild type. In *MHC-II*$^{-/-}$mice, there was a 3-log difference. Although the profound attenuation of the Δ*esxH* mutant is probably multifactorial, reflecting its role in metal homeostasis, phagosome maturation arrest and potentially other processes, the observation that there was a greater impact of T cells on the Δ*esxH* mutant than on H37Rv (Fig. 6c) is consistent with

the idea that the *in vivo* attenuation of Δ*esxH* depends in part on MHC-II-mediated antigen presentation and $CD4^+$ T-cell responses.

Discussion

We showed previously that to promote its intracellular survival Mtb secretes EsxH and inhibits the function of ESCRT. The role of ESCRT in antigen presentation has not previously been established. Here, we showed that ESCRT contributes to optimal antigen processing and that Mtb EsxH impairs the activation of $CD4^+$ T cells and their ability to promote bacterial clearance. Macrophages and DCs infected with an Mtb mutant lacking EsxH yielded enhanced T-cell activation, whereas infection with a strain that overexpressed $EsxGH_{Mt}$ elicited diminished T-cell responses. Overexpression of $EsxGH_{Ms}$, which does not bind HRS or inhibit ESCRT[20], had no effect on T-cell responses. Thus, the ability of $EsxGH_{Mt}$ to inhibit antigen presentation is probably due to a direct effect on HRS[20], although additional targets may also play a role. Our findings are in accordance with those of Tufariello *et al.*[26] who demonstrated an important role of *esxH* in virulence that is separable from the role in iron acquisition and that cannot be complemented by *esxG–esxH* from *M. smegmatis.*

This study is also, to the best of our knowledge, the first demonstration that ESCRT is required for antigen presentation. In DCs, degradation of peptide-loaded MHC-II is regulated by ubiquitination[31,32], which has been presumed to be ESCRT dependent. Based on the presumption that ESCRT regulates MHC-II degradation, we expected that ESCRT silencing would result in enhanced MHC-II surface expression and potentially increased antigen presentation. Rather, we found that silencing ESCRT impaired T-cell activation by inhibiting antigen processing and presentation. There are several ways in which ESCRT might do this. First, the multivesicular architecture of the MHC-II compartment might be important for the processing and/or loading of antigen[37–39]. Alternatively, given the role of ESCRT in phagosome maturation[20,29], ESCRT might promote antigen processing because it assists in trafficking Mtb to an acidic phagosomal environment that contains active lysosomal hydrolases. However, the literature does not suggest a simple relationship between phagosome maturation arrest, bacterial fitness and antigen presentation, as some attenuated strains are reported to enhance antigen presentation, whereas others have no effect[10,11,40–42]. Further complicating this explanation is the fact that lysosomal trafficking of Mtb in IFN-γ-activated macrophages does not depend on ESCRT (Supplementary Fig. 2). Nonetheless, there may be other aspects of the phagosomal environment that are altered by ESCRT inhibition, an explanation that we favour. For example, ESCRT might be required for trafficking the antigen processing or loading machinery to the phagolysosome or the MHC-II compartment.

Our findings extend well beyond the role of ESCRT in antigen presentation. To the best of our knowledge, this is the first example of an Mtb effector and its corresponding cellular target impairing MHC-II antigen presentation by a mechanism other than Mtb Toll-like receptor 2 agonists blocking IFN-γ signalling. The previously described mechanism cannot explain how Mtb downregulates antigen presentation in antigen-presenting cells that already express MHC-II or in macrophages that are exposed to IFN-γ shortly after they are infected.

Here, we have provided a molecular explanation for how, in migratory DCs and IFN-γ-activated macrophages, Mtb blunts T-cell responses. $EsxGH_{Mt}$ may provide a double hit for Mtb by impairing efficient priming of antigen-specific T cells and preventing effector $CD4^+$ T cells from recognizing infected macrophages, which is important for control of Mtb *in vivo*[36]. Importantly, this mechanism of immune evasion may also undermine the ability of pre-existing $CD4^+$ T cells generated by a vaccine or prior infection to be protective. Our results demonstrated only a partial suppression of T-cell activation in response to ESCRT silencing or *esxH* expression by the bacilli. Thus, there are likely to be additional mechanisms that Mtb uses to impair antigen presentation.

The observation that $EsxGH_{Mt}$ impairs antigen presentation would seem to be at odds with the findings that $EsxG_{Mt}$ and $EsxH_{Mt}$, also known as TB9.8 and TB10.4, respectively, are prominent T-cell antigens[43,44]. This apparent conundrum may be explained by the fact that antigen transfer from infected to uninfected DCs allows priming of T cells in the lymph node[18,19]. When these T cells arrive in the lung, the $EsxGH_{Mt}$-imposed block in antigen presentation in infected macrophages would subvert effector responses. This is an important consideration in vaccine candidates that include EsxH; macrophages infected with Mtb expressing abundant EsxH might be those that are imperceptible to $CD4^+$ T cells. Interestingly, a recent study found that EsxA/ESAT-6, secreted by the Esx-1 type VII secretion system, interacts with β_2-microglobulin and inhibits MHC class I β_2-microglobulin surface expression[45]. Thus, two of the most dominant T-cell antigens, EsxA and EsxH, appear to undermine the activation of two major T-cell subsets, leading us to speculate that their prominence as T-cell antigens reflects a bacterial strategy to generate an ineffective host response.

In conclusion, we have shown that ESCRT stimulates antigen presentation and that Mtb $EsxGH_{Mt}$ undermines this critical function in activated macrophages and DCs. Our data provide a molecular explanation for the failure of the adaptive immune response to kill Mtb. Recent work has shown that it is possible to identify small molecules that impair type VII secretion[46]. Esx-3 inhibitors could be particularly potent, as inhibiting this system would impair intrinsic bacterial processes involved in metal homeostasis, as well as promoting host clearance by restoring macrophage function and T-cell activation.

Methods

Mice

P25TCR-Tg[30] mice were bred into a C57BL/6 (CD45.1) background. C7TCR-Tg[47] mice have been described previously. C57BL/6 (CD45.2) and *MHC-II*$^{-/-}$ mice were purchased from The Jackson Laboratory. The New York University School of Medicine Institutional Animal Care and Use Committee approved all work with animals.

Bacterial strains and growth conditions

Mtb H37Rv overexpressing $EsxGH_{Mt}$ or $ESXGH_{MS}$, Mtb H37Rv expressing green fluorescent protein (GFP)[20], Δ*fbpB*[1], Δ*esxA*[48], $mc^2$7846 (Δ*esxH*) and $mc^2$7848 (Δ*pe5-ppe4*)[26] have been described previously. Mtb was grown at 37 °C to log phase in BD Difco

Middlebrook 7H9 (Fisher Scientific) medium with 0.05% Tween 80, BD BBL Middlebrook OADC Enrichment (Fisher Scientific) and 0.2% glycerol. The pJP130 complementing plasmid described below (Δ*esxH*-compl) and the GFP plasmids were selected with 25 μg ml^{-1} kanamycin (Sigma). Mycobactin was not used routinely to supplement the mutants during growth in broth culture. When plating for determination of c.f. u., the Δ*esxH* mutant was grown on 7H10 plates supplemented with 200 ng/ml mycobactin J (Allied Monitor).

Tissue culture

RAW264.7 cells were grown in DMEM (Gibco) with 10% heat-inactivated fetal bovine serum (FBS) and 2 mM L-glutamine. RAW264.7 cells were obtained from the American Type Culture Collection, and were expanded and frozen. After thawing, they were used within the first several passages and not tested for mycoplasma contamination. Bone marrow was isolated from 6–8-week-old male C57BL/6 mice as described previously[49] and cultured in BMMO medium (DMEM with 10% heat-inactivated FBS, 2 mM L-glutamine, 1 mM sodium pyruvate and 20% L929 cell-conditioned medium). BMDMs were collected between 6 and 7 d, detached from plates by incubation in ice-cold PBS with 5 mM EDTA, and then washed and plated in BMMO medium with 10% L929 cell-conditioned medium. Penicillin/streptomycin (Gibco) was added to the medium for passaging but omitted during infections. BMDCs were grown in RPMI 1640 with 10% heat-inactivated FBS, 2 mM L-glutamine, 1 mM sodium pyruvate, 1× β-mercaptoethanol (Gibco), 10 mM HEPES and 10 ng ml^{-1} recombinant murine granulocyte-macrophage colony-stimulating factor (Peprotech) for 7 d, followed by sorting of $CD11c^+$ DCs using magnetic cell sorting (autoMACS; Miltenyi Biotec).

siRNA treatment

Hiperfect (Qiagen) was used to transfect siRNAs 2 or 3d before infection of RAW cells or BMDMs, respectively.

$CD4^+$ T-cell isolation

P25[1,30] and C7TCR-Tg[47] T_H1 effector cells were generated *in vitro* as described previously. Briefly, $CD4^+$ T cells were isolated magnetically from lymph node cell suspensions from P25TCR-Tg and C7TCR-Tg mice using microbeads (MACS) and an autoMACS (both from Miltenyi Biotec). The cells were co-cultured with irradiated C57BL/6 splenocytes in the presence of mouse interleukin (IL)-12p70, IL-2, anti-IL-4 neutralizing antibody, and peptide P25 or ESAT-$6_{(1–20)}$ for 3 d and frozen until used.

Antigen presentation assays

At 7d after collection, 1×10^5 BMDMs per well were plated in 96-well plates and transfected with siRNAs. Two days later, they were treated with 200 U ml^{-1} IFN-γ (Gibco). The following day, they were infected with a single-cell suspension of Mtb (multiplicity of infection (m.o.i.) of 1–5) prepared as described previously[20]. After 4 h, extracellular bacteria were removed by washing three times with warm PBS. Infected macrophages were incubated at 37 °C for an additional 20 h, after which P25TCR T_H1 or C7TCR-Tg $CD4^+$ T cells were added (5×10^5 cells per well). At 24 h after co-culture of infected BMDMs with

$CD4^+$ T cells, culture supernatants were collected, filtered and assayed for IFN-γ by an enzyme-linked immunosorbent assay (ELISA: BD Biosciences). Alternatively, the antigen presentation assay was performed as above but without knocking down ESCRT, or, instead of infection with live Mtb, BMDMs were incubated with 0.5 μM P25 peptide or 10 μg ml^{-1} recombinant Ag85B protein (BEI Resources). Antigen presentation assays were also done using BMDCs as antigen-presenting cells. In this case, cells were not treated with IFN-γ before infection.

DQ-OVA processing assay

BMDMs were treated with 50 μg ml^{-1} DQ-OVA (Molecular Probes) for 30 min at 37 °C and washed three times with ice-cold PBS, followed by incubation in fresh medium at 37 °C for 24 h, after which they were fixed with 4% paraformaldehyde (PFA). Nuclei were stained with 2.5 μg ml^{-1} Hoechst 33342 (Molecular Probes). Images were captured using a Nikon Eclipse TiE/B automated fluorescent microscope with a Photometrics HQ@ Monochrome digital camera. *Z*-stack images were acquired at a magnification of ×60, and the mean fluorescence intensity (fluorescein isothiocyanate) was quantified using NIS-Elements DUO software.

Lysosomal trafficking assay

siRNA-transfected RAW cells or BMDMs were infected with GFP-expressing Mtb for 4 h as described above. One day before infection, macrophages were treated with IFN-γ (100 U ml^{-1}) or left untreated. Cells were fixed with 1% PFA in PBS overnight at 24 h postinfection, permeabilized with 0.1% saponin in PBS and blocked with 2% BSA in PBS for 1 h. Cells were then immunostained for LAMP1 (1:1000 dilution; Abcam) for at least 1 h at room temperature or at 4 °C overnight, followed by treatment with anti-rabbit Alexa Fluor 594-conjugated secondary antibody (Invitrogen). Images were captured using a Nikon Eclipse TiE/B automated fluorescent microscope described above and analysed using NIS-Elements DUO software as described previously[20].

Intracellular bacterial growth assay

RAW cells or BMDMs were transfected with siRNA and infected as described above (m.o.i. of 5). IFN-γ (100 U ml^{-1}) was added 1 d before infection. At 4 h or 2 d postinfection, the cells were lysed with 0.2% Triton X-100 and serial dilutions plated. The numbers of c.f.u. were calculated 15–21 d later. For co-culture experiments, BMDMs were infected with wild-type Mtb or Δ*esxH* mutant (m.o.i. of 3). At 24 h postinfection, P25TCR-Tg effector T cells were added or not, and 24 h later, cells were lysed, diluted and plated as described above at different time points.

Western blot analysis

BMDMs were transfected with siRNA for 72 h, after which cellular lysates were prepared in RIPA buffer with Halt Protease Inhibitor Cocktail (Thermo Scientific) and analysed by western blotting. The antibodies used for western blot analysis were against actin (clone C4; Millipore), HRS (M79; Santa Cruz Biotechnology) and TSG101 (Genetex).

Adoptive transfer and naive P25TCR-Tg CD4+ T-cell proliferation

CD4+ T cells (3×10^6) collected from the lymph nodes and spleens of female P25TCR-Tg mice (8–12 weeks old) were labelled with 10 μM CFSE for 7 min and adoptively transferred by retro-orbital injections into 8-week-old female recipient mice. After 24 h, recipient mice were infected with 2×10^2 c.f.u. H37Rv or 1×10^4 c.f.u. Δ*esxH* mutant by the aerosol route using an Inhalation Exposure Unit (Glas-Col), as described previously[15]. At 7, 14 and 21 d after infection, MLNs and lungs were obtained from recipient mice and cells were analysed for CFSE dilution by flow cytometry. The experiments were not randomized or blinded. The number of animals used was determined based on feasibility and prior experience with the assay.

Intratracheal transfer of infected BMDCs

BMDC from wild-type mice were infected overnight with H37Rv or Δ*esxH* (m.o.i. of 1), washed, treated with amikacin (200 pg ml^{-1} for 40 min) and administered intratracheally to *MHC-II*$^{-/-}$ mice (5×10^5 DCs per mouse) 1 d after adoptive transfer of CFSE-labelled naive P25TCR-Tg CD4 cells (4×10^6 cells per mouse). At 60 h after BMDC transfer, MLNs were collected and processed for determination of bacterial c.f.u. and flow cytometry, and the lungs were processed for determination of c.f.u.

Flow cytometry

BMDMs were fixed in 1% PFA and stained using Alexa Fluor 488-conjugated anti-mouse MHC-II (I-A/I-E, clone M5/114.15.2; Biolegend). Single-cell suspensions from infected lungs and MLNs were stained using the following fluorescently labelled antibodies: Alexa Fluor 700-conjugated anti-mouse CD45.1 antibody (clone A20), peridinin–chlorophyll-conjugated anti-mouse CD3e (clone 145-2C11) and Pacific Blue-conjugated anti-mouse CD4 antibody (clone RM4-5) (all from Biolegend). Flow cytometry was performed using a FACSCalibur and LSR II (BD Biosciences) at the New York University Cytometry and Cell Sorting Core. FlowJo software was used for data analysis.

Plasmids

pJP130 was used to complement the Δ*esxH* mutant. It was constructed by inserting *Rv0289* into pYUB1944, which contains *esxG–esxH* under control of the *hsp60* promoter[26]. *Rv0289* was amplified from Mtb genomic DNA by PCR using forward (5′-TAGAAGCTTCTCGCGCTACATGGATGC-3′) and reverse (5′-CCAATCGATTTACGAGGATTGGGTGG-3′) primers, digested with HindIII, and cloned into the HindIII site after *Rv0288* in pYUB1944. The addition of *Rv0289* to pYUB1944 resulted in enhanced secretion of EsxG and EsxH compared with the parental plasmid.

Mass spectrometry analysis

Triplicate samples of H37Rv and Δ*esxH* culture filtrate were prepared and analysed by liquid chromatography/tandem mass spectrometry using an Easy nLC-1000 on-line with a QExactive mass spectrometer (Thermo Scientific) as described[26]. The data was analysed with MaxQuant software with the Andromeda search engine for peptide identification.

Label-free quantitation algorithms were used to determine normalized relative protein quantitation values[50].

Statistical analysis

Biological and technical replicates were used for analyses. Data shown are representative of two or more independent experiments. In all figures, error bars indicate means ± s.e.m. An unpaired Student's *t*-test was used to determine statistical significance between experimental groups unless otherwise indicated.

Data availability

The data that support the findings of this study are available from the corresponding authors (W.R.J. and J.A.P.) on request.

Supplementary Material

Refer to Web version on PubMed Central for supplementary material.

Acknowledgments

We thank the New York University Cytometry Core at the Laura and Isaac Perlmutter Cancer Center (partially supported by a Cancer Center Support Grant, P30CA016087) for their assistance with flow cytometry, Beatrix Ueberheide and Jessica Chapman-Lim for assistance with proteomics (New York University Proteomics Resource Center), Michael Glickman (Memorial Sloan-Kettering Cancer Center) for the C7TCR Tg mice, BEI Resources, NIAID, NIH for Ag85B protein (Ag85B Recombinant Protein Reference Standard, NR-14870), and members of the Philips and Ernst laboratories, in particular Colette O'Shaughnessy and Ludovic Desvignes, for assistance and helpful discussions. This workwas supported by National Institutes of Health grants R01s AI087682, AI026170, and AI098925, K08 AI119150-01 and UL1 TR000038.

References

1. Wolf AJ, et al. Initiation of the adaptive immune response to *Mycobacterium tuberculosis* depends on antigen production in the local lymph node, not the lungs. J Exp Med. 2008; 205:105–115. [PubMed: 18158321]
2. MacMicking JD. Interferon-inducible effector mechanisms in cell-autonomous immunity. Nat Rev Immunol. 2012; 12:367–382. [PubMed: 22531325]
3. Fortune SM, et al. Mycobacterium tuberculosis inhibits macrophage responses to IFN-γ through myeloid differentiation factor 88-dependent and -independent mechanisms. J Immunol. 2004; 172:6272–6280. [PubMed: 15128816]
4. Noss EH, et al. Toll-like receptor 2-dependent inhibition of macrophage class II MHC expression and antigen processing by 19-kDa lipoprotein of *Mycobacterium tuberculosis*. J Immunol. 2001; 167:910–918. [PubMed: 11441098]
5. Pennini ME, Pai RK, Schultz DC, Boom WH, Harding CV. *Mycobacterium tuberculosis* 19-kDa lipoprotein inhibits IFN-γ-induced chromatin remodeling of MHC2TA by TLR2 and MAPK signaling. J Immunol. 2006; 176:4323–4330. [PubMed: 16547269]
6. Kincaid EZ, et al. Codominance of TLR2-dependent and TLR2-independent modulation of MHC class II in *Mycobacterium tuberculosis* infection in vivo. J Immunol. 2007; 179:3187–3195. [PubMed: 17709534]
7. Blander JM, Medzhitov R. On regulation of phagosome maturation and antigen presentation. Nat Immunol. 2006; 7:1029–1035. [PubMed: 16985500]
8. Ramachandra L, Noss E, Boom WH, Harding CV. Processing of *Mycobacterium tuberculosis* antigen 85B involves intraphagosomal formation of peptide-major histocompatibility complex II

complexes and is inhibited by live bacilli that decrease phagosome maturation. J Exp Med. 2001; 194:1421–1432. [PubMed: 11714749]

9. Jagannath C, et al. Autophagy enhances the efficacy of BCG vaccine by increasing peptide presentation in mouse dendritic cells. Nat Med. 2009; 15:267–276. [PubMed: 19252503]
10. Johansen P, et al. Relieffrom Zmp1-mediated arrest of phagosome maturation is associated with facilitated presentation and enhanced immunogenicity of mycobacterial antigens. Clin Vaccine Immunol. 2011; 18:907–913. [PubMed: 21471301]
11. Majlessi L, et al. Inhibition of phagosome maturation by mycobacteria does not interfere with presentation of mycobacterial antigens by MHC molecules. J Immunol. 2007; 179:1825–1833. [PubMed: 17641049]
12. Hanekom WA, et al. Mycobacterium tuberculosis inhibits maturation of human monocyte-derived dendritic cells in vitro. J Infect Dis. 2003; 188:257–266. [PubMed: 12854081]
13. Henderson RA, Watkins SC, Flynn JL. Activation of human dendritic cells following infection with *Mycobacterium tuberculosis*. J Immunol. 1997; 159:635–643. [PubMed: 9218578]
14. Giacomini E, et al. Infection of human macrophages and dendritic cells with *Mycobacterium tuberculosis* induces a differential cytokine gene expression that modulates T cell response. J Immunol. 2001; 166:7033–7041. [PubMed: 11390447]
15. Wolf AJ, et al. Mycobacterium tuberculosis infects dendritic cells with high frequency and impairs their function in vivo. J Immunol. 2007; 179:2509–2519. [PubMed: 17675513]
16. Grace PS, Ernst JD. Suboptimal antigen presentation contributes to virulence of *Mycobacterium tuberculosis* in vivo. J Immunol. 2016; 196:357–364. [PubMed: 26573837]
17. Samstein M, et al. Essential yet limited role for $CCR2^{+}$ inflammatory monocytes during *Mycobacterium tuberculosis-specific* T cell priming. eLife. 2013; 2:e01086. [PubMed: 24220507]
18. Srivastava S, Ernst JD. Cell-to-cell transfer of *M. tuberculosis* antigens optimizes CD4T cell priming. Cell Host Microbe. 2014; 15:741–752. [PubMed: 24922576]
19. Srivastava S, Grace PS, Ernst JD. Antigen export reduces antigen presentation and limits T cell control of *M. tuberculosis*. Cell Host Microbe. 2016; 19:44–54. [PubMed: 26764596]
20. Mehra A, et al. Mycobacterium tuberculosis type VII secreted effector EsxH targets host ESCRT to impair trafficking. PLoS Pathog. 2013; 9:e1003734. [PubMed: 24204276]
21. Serafini A, Pisu D, Palù G, Rodriguez GM, Manganelli R. The ESX-3 secretion system is necessary for iron and zinc homeostasis in *Mycobacterium tuberculosis*. PLoS ONE. 2013; 8:e78351. [PubMed: 24155985]
22. Serafini A, Boldrin F, Palù G, Manganelli R. Characterization of a *Mycobacterium tuberculosis* ESX-3 conditional mutant: essentiality and rescue by iron and zinc. J Bacteriol. 2009; 191:6340–6344. [PubMed: 19684129]
23. Siegrist MS, et al. Mycobacterial Esx-3 requires multiple components for iron acquisition. mBio. 2014; 5:e01073–14. [PubMed: 24803520]
24. Siegrist MS, et al. Mycobacterial Esx-3 is required for mycobactin-mediated iron acquisition. Proc Natl Acad Sci USA. 2009; 106:18792–18797. [PubMed: 19846780]
25. Tinaztepe E, et al. Role of metal-dependent regulation of ESX-3 secretion in intracellular survival of *Mycobacterium tuberculosis*. Infect Immun. 2016; 84:2255–2263. [PubMed: 27245412]
26. Tufariello JM, et al. Separable roles for *Mycobacterium tuberculosis* ESX-3 effectors in iron acquisition and virulence. Proc Natl Acad Sci USA. 2016; 113:E348–E357. [PubMed: 26729876]
27. Sweeney KA, et al. A recombinant *Mycobacterium smegmatis* induces potent bactericidal immunity against *Mycobacterium tuberculosis*. Nat Med. 2011; 17:1261–1268. [PubMed: 21892180]
28. Raiborg C, Stenmark H. The ESCRT machinery in endosomal sorting of ubiquitylated membrane proteins. Nature. 2009; 458:445–452. [PubMed: 19325624]
29. Philips JA, Porto MC, Wang H, Rubin EJ, Perrimon N. ESCRT factors restrict mycobacterial growth. Proc Natl Acad Sci USA. 2008; 105:3070–3075. [PubMed: 18287038]
30. Tamura T, et al. The role of antigenic peptide in $CD4^{+}$ T helper phenotype development in a T cell receptor transgenic model. Int Immunol. 2004; 16:1691–1699. [PubMed: 15477229]

31. Baravalle G, et al. Ubiquitination of CD86 is a key mechanism in regulating antigen presentation by dendritic cells. J Immunol. 2011; 187:2966–2973. [PubMed: 21849678]
32. Ohmura-Hoshino M, et al. Cutting edge: requirement of MARCH-I-mediated MHC II ubiquitination for the maintenance of conventional dendritic cells. J Immunol. 2009; 183:6893–6897. [PubMed: 19917682]
33. Via LE, et al. Arrest of mycobacterial phagosome maturation is caused by a block in vesicle fusion between stages controlled by rab5 and rab7. J Biol Chem. 1997; 272:13326–13331. [PubMed: 9148954]
34. Gutierrez MG, et al. Autophagy is a defense mechanism inhibiting BCG and *Mycobacterium tuberculosis* survival in infected macrophages. Cell. 2004; 119:753–766. [PubMed: 15607973]
35. Sakowski ET, et al. Ubiquilin 1 promotes IFN-γ-induced xenophagy of *Mycobacterium tuberculosis*. PLoS Pathogens. 2015; 11:e1005076. [PubMed: 26225865]
36. Srivastava S, Ernst JD. Cutting edge: direct recognition of infected cells by CD4T cells is required for control of intracellular *Mycobacterium tuberculosis* in vivo. J Immunol. 2013; 191:1016–1020. [PubMed: 23817429]
37. Ten Broeke T, Wubbolts R, Stoorvogel W. MHC class II antigen presentation by dendritic cells regulated through endosomal sorting. Cold Spring Harb Perspect Biol. 2013; 5:a016873. [PubMed: 24296169]
38. Zwart W, et al. Spatial separation of HLA-DM/HLA-DR interactions within MIIC and phagosome-induced immune escape. Immunity. 2005; 22:221–233. [PubMed: 15723810]
39. Bosch B, et al. Disruption of multivesicular body vesicles does not affect major histocompatibility complex (MHC) class II-peptide complex formation and antigen presentation by dendritic cells. J Biol Chem. 2013; 288:24286–24292. [PubMed: 23846690]
40. Singh CR, et al. Processing and presentation of a mycobacterial antigen 85B epitope by murine macrophages is dependent on the phagosomal acquisition of vacuolar proton ATPase and in situ activation of cathepsin D. J Immunol. 2006; 177:3250–3259. [PubMed: 16920965]
41. Hinchey J, et al. Enhanced priming of adaptive immunity by a proapoptotic mutant of *Mycobacterium tuberculosis*. J Clin Invest. 2007; 117:2279–2288. [PubMed: 17671656]
42. Saikolappan S, et al. The *fbpA*/*sapM* double knock out strain of *Mycobacterium tuberculosis* is highly attenuated and immunogenic in macrophages. PLoS ONE. 2012; 7:e36198. [PubMed: 22574140]
43. Hervas-Stubbs S, et al. High frequency of $CD4^+$ T cells specific for the TB10.4 protein correlates with protection against *Mycobacterium tuberculosis* infection. Infect Immun. 2006; 74:3396–3407. [PubMed: 16714570]
44. Skjot RL, et al. Epitope mapping of the immunodominant antigen TB10.4 and the two homologous proteins TB10.3 and TB12.9, which constitute a subfamily of the *esat-6* gene family. Infect Immun. 2002; 70:5446–5453. [PubMed: 12228269]
45. Sreejit G, et al. The ESAT-6 protein of *Mycobacterium tuberculosis* interacts with beta-2-microglobulin (β2M) affecting antigen presentation function of macrophage. PLoS Pathog. 2014; 10:e1004446. [PubMed: 25356553]
46. Rybniker J, et al. Anticytolytic screen identifies inhibitors of mycobacterial virulence protein secretion. Cell Host Microbe. 2014; 16:538–548. [PubMed: 25299337]
47. Gallegos AM, Pamer EG, Glickman MS. Delayed protection by ESAT-6-specific effector $CD4^+$ T cells after airborne *M. tuberculosis* infection. J Exp Med. 2008; 205:2359–2368. [PubMed: 18779346]
48. Wong KW, Jacobs WR Jr. Critical role for NLRP3 in necrotic death triggered by *Mycobacterium tuberculosis*. Cell Microbiol. 2011; 13:1371–1384. [PubMed: 21740493]
49. Banaiee N, Kincaid EZ, Buchwald U, Jacobs WR Jr, Ernst JD. Potent inhibition of macrophage responses to IFN-γ by live virulent *Mycobacterium tuberculosis* is independent of mature mycobacterial lipoproteins but dependent on TLR2. J Immunol. 2006; 176:3019–3027. [PubMed: 16493060]
50. Luber CA, et al. Quantitative proteomics reveals subset-specific viral recognition in dendritic cells. Immunity. 2010; 32:279–289. [PubMed: 20171123]

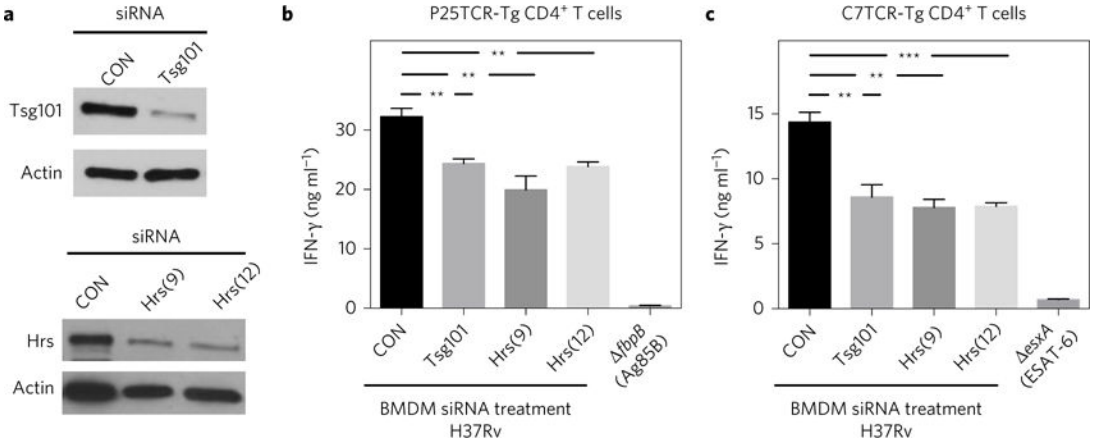

Figure 1. ESCRT promotes antigen presentation by Mtb-infected macrophages

a, BMDMs were transfected with small interfering RNA (siRNA) pools targeting *Tsg101*, individual siRNAs targeting *Hrs* (numbers 9 and 12) or a non-targeting control (CON). After 96 h, the lysates were analysed by western blotting. Actin served as a loading control. Images shown are from one experiment, representative of at least three independent experiments. **b**,**c**, BMDMs were treated with siRNAs as indicated and infected 3 d later with Mtb H37Rv (multiplicity of infection of 3–5), Δ*fbpB* or Δesx*A* strain. The following day, infected BMDMs were co-cultured for 24 h with P25TCR-Tg (**b**) or C7TCR-Tg (**c**) $CD4^+$ T cells, and IFN-γ was measured from culture supernatants by an enzyme-linked immunosorbent assay (ELISA). Results reflect the mean ± s.e.m. from at least four replicates and are representative of at least three independent experiments. $^{**}P = 0.005$, $^{***}P = 0.0001$ (unpaired Student's *t*-test).

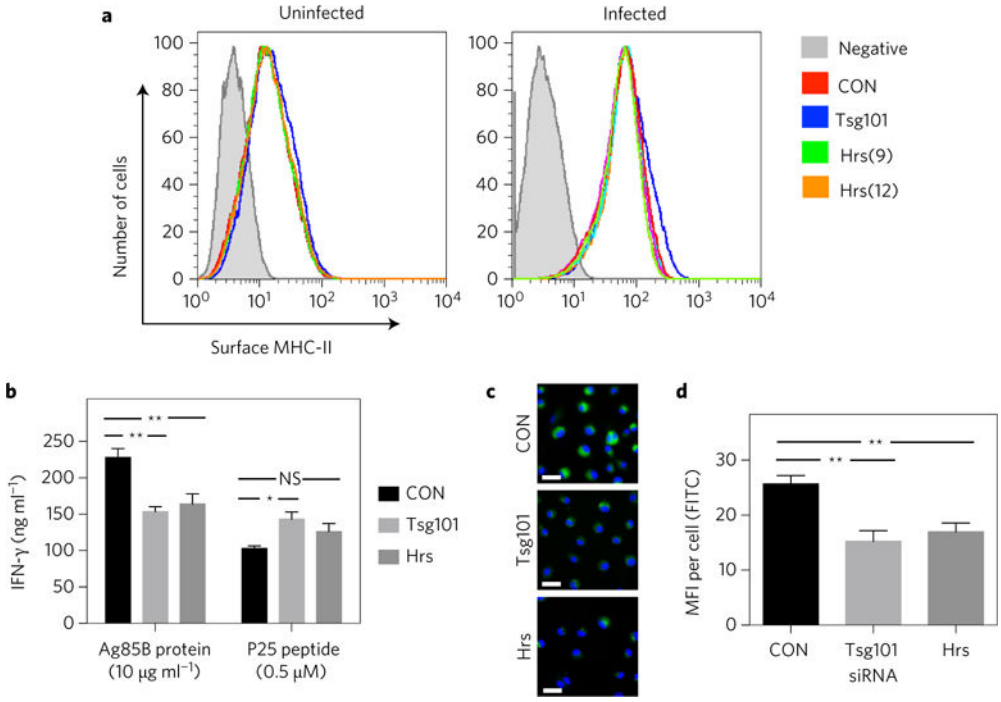

Figure 2. ESCRT promotes antigen presentation by facilitating antigen processing

a–d, BMDMs were treated with siRNAs targeting *Hrs* (numbers 9 and 12 in panel **a**, number 9 in **b–d**) or *Tsg101* (pool). (**a**) Mtb-infected and uninfected BMDMs were immunostained with anti-mouse MHC-II (I-A/I-E) and analysed by flow cytometry. Shaded histograms indicate unstained controls. Data are representative of two independent experiments. (**b**) BMDMs were incubated with recombinant Ag85B protein or peptide P25 and co-cultured with P25TCR-Tg T cells. IFN-γ was measured by ELISA. Results reflect means ± s.e.m. from at least three replicates. (**c**) BMDMs were treated with DQ-OVA and the level of green fluorescence was determined using fluorescence microscopy. Images presented are representative of three independent experiments. FITC, fluorescein isothiocyanate. Scale bars, 20 μm. **d**, Graph shows means ± s.e.m. of the mean fluorescence intensity (MFI) of at least 50 cells for each condition. $*P < 0.05$, $**P < 0.01$ (unpaired Student's *t*-test); NS, not significant.

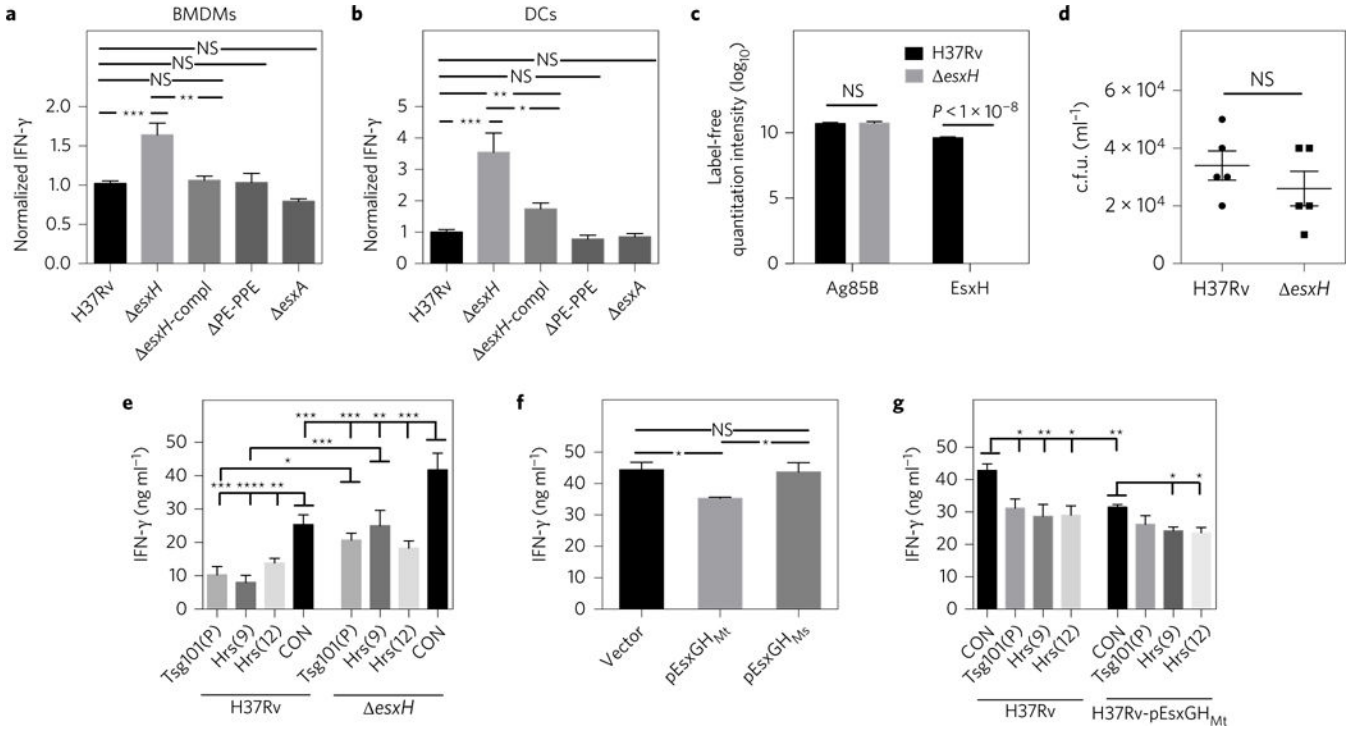

Figure 3. EsxGH$_{Mt}$ impairs antigen presentation

a,**b**, BMDMs (**a**) or DCs (**b**) were infected with Mtb H37Rv, Δ*esxH* (mc^{2}7846), Δ*esxH* complemented with EsxGH (Δ*esxH*-compl), Δ*pe5ppe4* (mc^{2}7848; ΔPE-PPE) or Δ*esxA*, and co-cultured with P25TCR-Tg CD4$^+$ T cells. Results were normalized to H37Rv infection from at least three independent experiments and reflect means ± s.e.m. **c**, Mass spectrometry and label-free quantitation algorithms were used to determine normalized relative protein levels of Ag85B and EsxH in culture filtrate from the wild type and the Δ*esxH* mutant[26]. Results are combined from three independent experiments and reflect means ± s.e.m. **d**, Bacterial burden in H37Rv- or Δ*esxH*-infected BMDMs at 24 h postinfection. Results are representative of two independent experiments and reflect means ± s.e.m. **e**, BMDMs were treated with siRNA and infected with either H37Rv or Δ*esxH* and co-cultured with P25TCR-Tg CD4$^+$ T cells as above. One-way analysis of variance (ANOVA) was used to compare the siRNA control (CON) sample with ESCRT-silenced samples for both H37Rv and Δ*esxH* infection. For each siRNA, H37Rv was compared with Δ*esxH*. Results are representative of three independent experiments and reflect means ± s.e.m. All significant results are indicated, **f**, BMDMs were infected with H37Rv containing empty vector, EsxGH$_{Mt}$ or EsxGH$_{Ms}$ for 24 h and co-cultured with P25TCR-Tg CD4$^+$ effector T cells. Results are representative of two independent experiments and reflect means ± s.e.m. **g**, BMDMs were treated with the indicated siRNAs and infected with Mtb containing empty vector or EsxGH$_{Mt}$ as indicated and co-cultured with P25TCR-Tg CD4$^+$ T cells. One-way ANOVA was used to compare the siRNA control sample with ESCRT-silenced samples for both vector control and EsxGH$_{Mt}$; the vector control strain was compared with the EsxGH$_{Mt}$ strain for each siRNA treatment. Results are representative of three independent experiments and reflect means ± s.e.m. All significant differences are indicated. For **a**,**b**,**e–g**, IFN-γ

released into culture supernatants was measured by an ELISA. *P <0.05, **P<0.01, ***P<0.005, ****P <0.0001 (unpaired Student's t-test); NS, not significant.

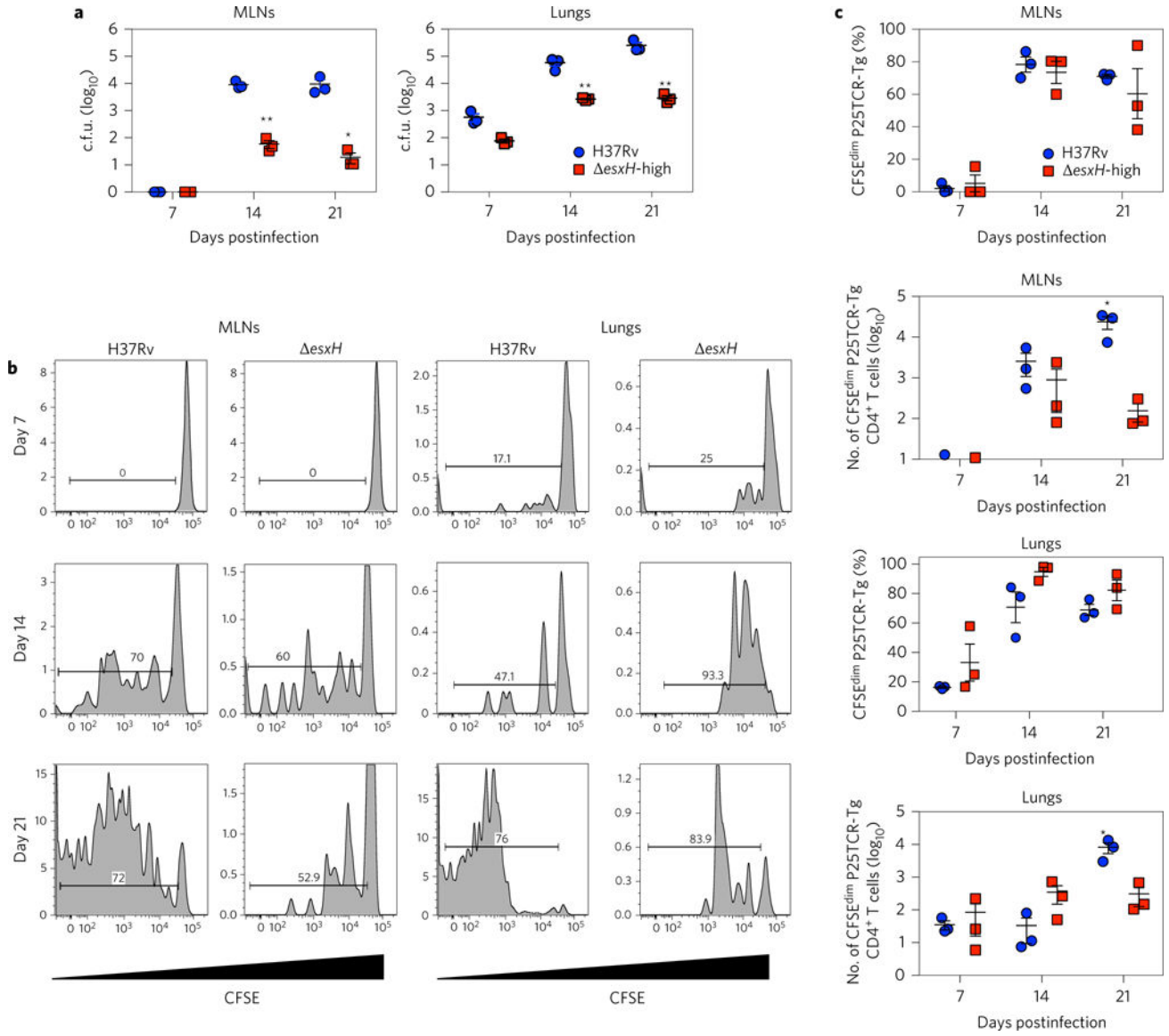

Figure 4. Fewer Δ*esxH* c.f.u. are required to initiate proliferation in the MLNs and lungs

Mice with adoptively transferred CFSE-labelled P25TCR-Tg CD4$^+$ T cells were infected by aerosol with H37Rv or high-dose Δ*esxH*. **a**, The number of c.f.u. in the MLNs and lungs was quantified at the indicated times (n = 3 mice per time point for each bacterial strain). Results reflect means ± s.e.m. **b**, Representative CFSE dilution profiles of adoptively transferred CFSE-labelled P25TCR-Tg CD4$^+$ T cells in the MLNs and lung at different time points after aerosol infection. The y axis indicates the number of events. The horizontal bar indicates the percentage of proliferating cells. **c**, Quantitation of proliferating P25TCR-Tg CD4$^+$ T cells in the MLNs and lungs after infection with H37Rv or Δ*esxH*, as determined by flow cytometry. Results reflect means ± s.e.m. Results are representative of two similar experiments. *P< 0.05, **P < 0.01 (unpaired Student's t-test).

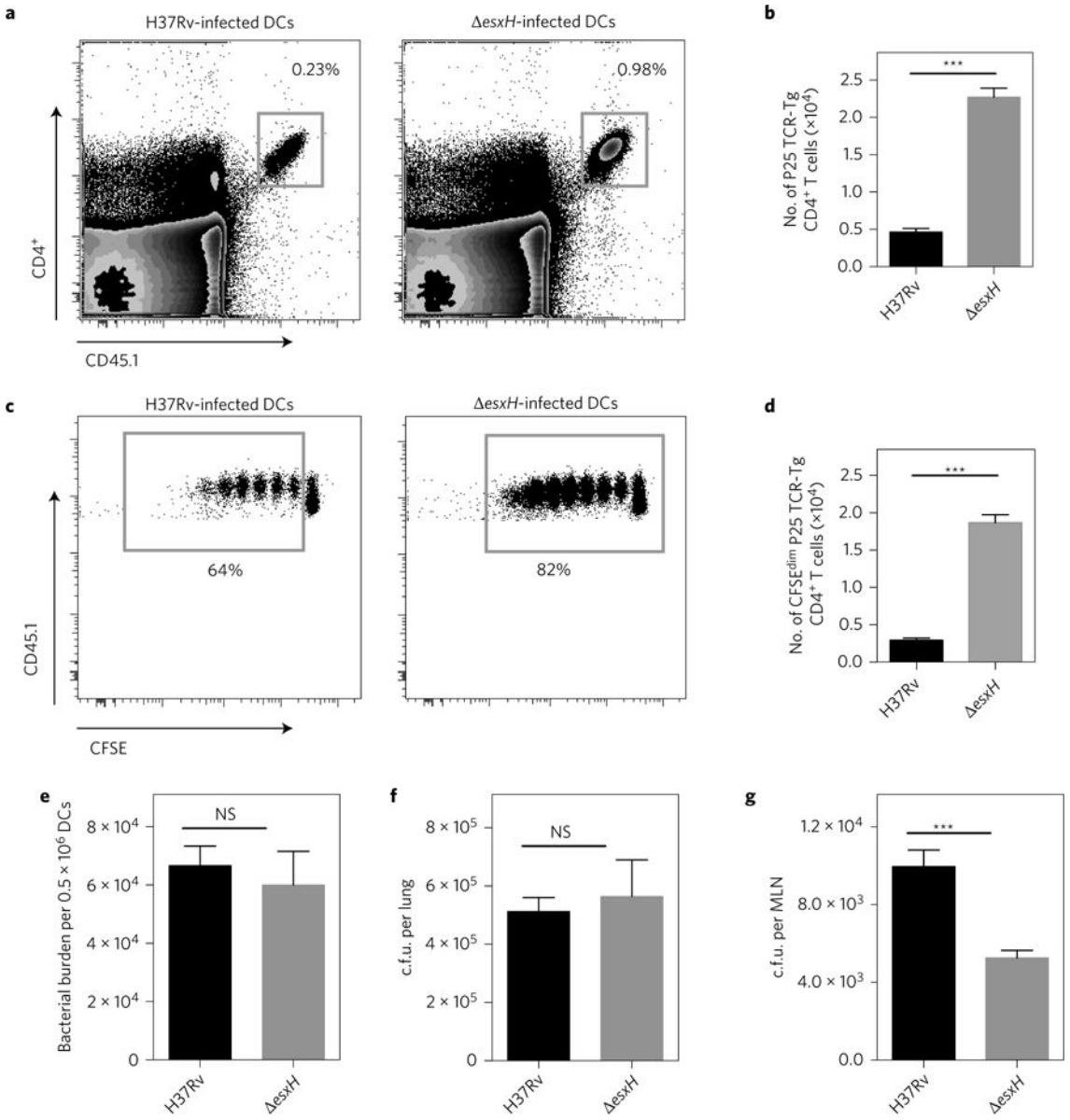

Figure 5. EsxGH$_{Mt}$ impairs priming of naive CD4$^+$ T cells *in vivo*

a, Representative fluorescence-activated cell sorting plots showing the frequency of adoptively transferred P25TCR-Tg CD4$^+$ T cells in the MLNs of *MHC-II*$^{-/-}$ mice 60 h after intratracheal transfer of *MHC-II*$^{+/+}$ DCs infected with either H37Rv or *ΔesxH.* **b**, Quantitation of total P25TCR-Tg CD4$^+$ T cells in the MLNs of the groups of mice shown in (**a**). **c**, Frequency of CFSE-labelled P25TCR-Tg CD4$^+$ T cells undergoing proliferation in the MLNs of mice 60 h after intratracheal transfer of either H37Rv- or Δ*esxH*-infected *MHC-II*$^{+/+}$ DCs. **d**, Quantitation of P25TCR-Tg CD4$^+$ T cells that have undergone at least one cycle of proliferation (CFSE^{dim}) in MLNs of groups of mice shown in **a–c**. **e**, Bacterial burden in H37Rv- or Δ*esxH*-infected BMDCs used for intratracheal transfer. Data are expressed as means ± s.e.m. of infected BMDCs in three replicates. **f**,**g**, Bacterial burden in lungs **f** or MLNs **g** of mice 60 h after receiving intratracheal BMDCs infected with either

H37Rv or Δ*esxH*. All data are from one experiment expressed as mean ± s.e.m. of three pools of mice ($n = 6$) per experimental group. ***$P < 0.001$ (Student's *t*-test); NS, not significant.

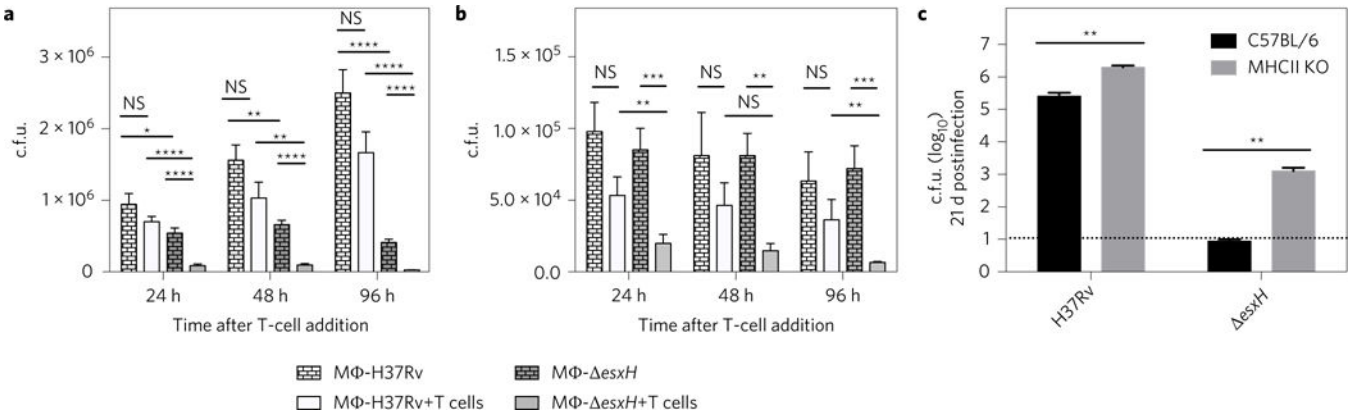

Figure 6. EsxH protects Mtb from CD4$^+$ T-cell mediated killing

a, BMDMs infected with H37Rv (wild type) or Δ*esxH* for 24 h were cultured for an additional 96 h in the absence or presence of P25TCR-Tg CD4$^+$ cells as indicated, and the number of c.f.u. was determined. **b**, BMDMs treated with IFN-γ (activated BMDMs) the day before they were infected with H37Rv (wild type) or Δ*esxH* were incubated at 24 h postinfection with or without P25TCR-Tg CD4$^+$ cells, and the number of c.f.u. was determined at the indicated time points. Data in **a** and **b** are expressed as means ± s.e.m. from two independent experiments with at least eight individual replicates per experimental group. *P<0.05, **P<0.01, ***P<0.001, ****P<0.0001 (Student's t-test corrected for multiple comparisons using the Holm-Sidak method). **c**, C57BL/6 and MHC-II KO mice were infected with H37Rv or Δ*esxH* by aerosol (10^2 c.f.u. for both strains), and the number of c.f.u. was determined in the lungs at 21 d postinfection. Dashed horizontal line indicates the limit of detection. Data are from one experiment expressed as means ± s.e.m. (n = 5 per group). **P <0.01 (unpaired Student's t-test). MΦ, macrophage; KO, knockout.